A Modified Beam-to-Earth Transformation to Measure Short-Wavelength Internal Waves with an Acoustic Doppler Current Profiler

A. SCOTTI

Department of Marine Sciences, University of North Carolina at Chapel Hill, Chapel Hill, North Carolina

B. BUTMAN

U.S. Geological Survey, Woods Hole, Massachusetts

R. C. BEARDSLEY

Department of Physical Oceanography, Woods Hole Oceanographic Institution, Woods Hole, Massachusetts

P. SOUPY ALEXANDER

U.S. Geological Survey, Woods Hole, Massachusetts

S. ANDERSON

Horizon Marine, Inc., Marion, Massachusetts

(Manuscript received 19 March 2004, in final form 10 September 2004)

ABSTRACT

The algorithm used to transform velocity signals from beam coordinates to earth coordinates in an acoustic Doppler current profiler (ADCP) relies on the assumption that the currents are uniform over the horizontal distance separating the beams. This condition may be violated by (nonlinear) internal waves, which can have wavelengths as small as 100–200 m. In this case, the standard algorithm combines velocities measured at different phases of a wave and produces horizontal velocities that increasingly differ from true velocities with distance from the ADCP. Observations made in Massachusetts Bay show that currents measured with a bottom-mounted upward-looking ADCP during periods when short-wavelength internal waves are present differ significantly from currents measured by point current meters, except very close to the instrument. These periods are flagged with high error velocities by the standard ADCP algorithm. In this paper measurements from the four spatially diverging beams and the backscatter intensity signal are used to calculate the propagation direction and celerity of the internal waves. Once this information is known, a modified beam-to-earth transformation that combines appropriately lagged beam measurements can be used to obtain current estimates in earth coordinates that compare well with pointwise measurements.

1. Introduction

The introduction of the acoustic Doppler current profiler (ADCP) in the late 1980s represented a major step forward in ocean technology, allowing effective remote sensing of ocean currents. To maintain a good signal-to-noise ratio, the acoustic beams spread radially at an angle from the vertical, which, depending on the instrument, varies between 15° and 30°. Thus, the velocity information derived from the Doppler shift within each beam is a combination of the horizontal and vertical components of the velocity in the sampling bin. To recover the velocity components in earth coordinates, the ADCP algorithm assumes that the current field is spatially uniform over the distance separating the beams, and combines data from opposite beams to determine the horizontal and vertical components. In most ocean applications, the assumption of local homogeneity is not a severe constraint, because the horizontal length scale of the phenomenon giving rise to the observed velocity distribution is usually much larger than the beam separation, which grows linearly with increasing distance from the instrument transducers (e.g., reaching 73 m in 100 m of water for a 20° beam angle). The error velocity, proportional to the differ-

Corresponding author address: A. Scotti, University of North Carolina at Chapel Hill, CB 3300, Chapel Hill, NC 27599-3300.
E-mail: ascotti@unc.edu

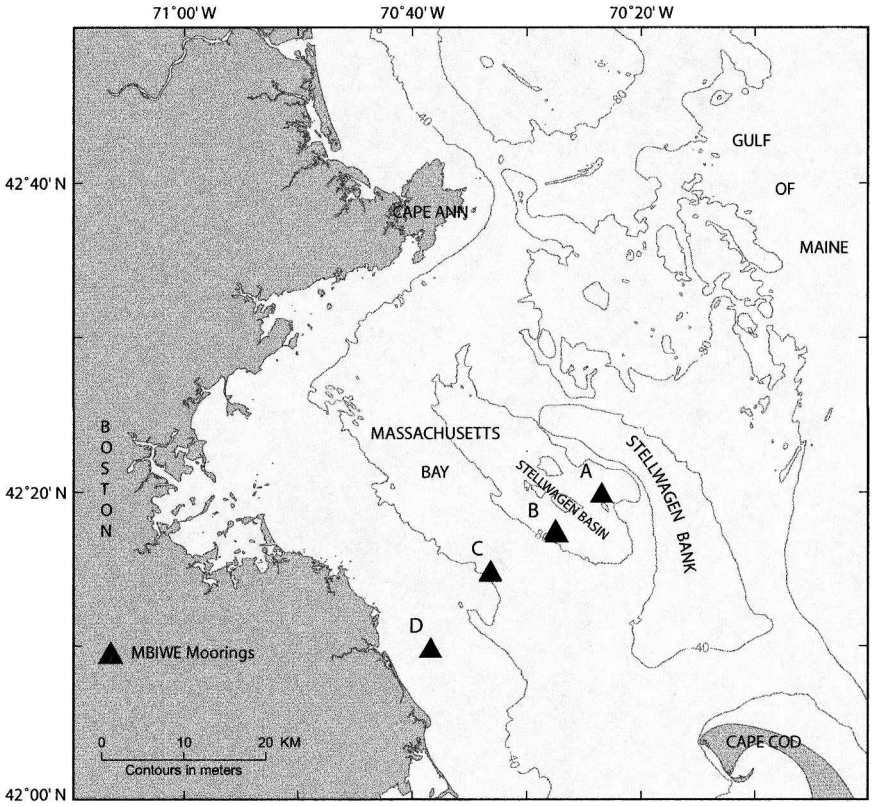

FIG. 1. Sites occupied during MBIWE98. The data used in the present analysis were collected at site B.

ence between the vertical velocities estimated from each pair of beams, can be used to flag situations where local homogeneity is violated.

In this paper, we address measurement of currents generated by packets of short-wavelength internal waves (SWIWs), which violate the condition of local homogeneity. Because of the renewed interest in this type of waves, especially in coastal areas (Colosi et al. 2001; Holloway et al. 2001; Holt and Thorpe 1997; Liu et al. 1998; New and Pingree 1992; Small et al. 1999; Trevorrow 1998), it is important to understand the nature of the error introduced by violations to the local homogeneity condition and, if possible, to devise ways to correct it. The observations presented here were made in August 1998 during the Massachusetts Bay Internal Wave Experiment (MBIWE98). This field experiment was designed to observe the propagation of SWIWs across Massachusetts Bay and utilized an array of instruments [including ADCPs, vector measuring current meters (VMCMs), and acoustic current meters (ACMs)] to measure currents at two locations (sites B and C in Fig. 1). Comparison of these observations showed significant differences between the ADCP and point current meter observations and led to the analysis presented here.

This paper is organized as follows. In section 2 we set up the problem and we define the local homogeneity condition. In section 3 we consider examples from data collected in Massachusetts Bay. In section 4 we show that, provided the celerity of the waves is known, it is possible to modify the beam-to-earth transformation to account for violations of the local homogeneity condition. We also introduce a method to calculate the celerity based on the cross correlation of the intensity of the backscattered energy from different beams. In section 5, we apply the modified algorithm to the Massachusetts Bay data, and we show that the corrected velocity signals compare well with pointwise measurements. Discussion and summary are presented in section 6.

2. Potential errors in measuring internal waves using ADCPs

The spatial filtering effects of four-beam ADCPs have been discussed in the literature in the context of turbulence measurements (Gargett 1994) and internal wave spectra (Polzin et al. 2002). Here we apply similar ideas to internal waves with a defined modal structure. The velocity field generated by a plane internal wave propagating in the east–west (E–W)(x) direction can be written as

$$u = u_a(z)f[k(x + Vt)] + u_o$$

$$w = w_a(z)g[k(x + Vt)], \quad (1)$$

where $u_a(z)$ and $w_a(z)$ are depth-dependent coefficients and u_o is a background current. The celerity V is assumed independent of depth, which is usually the case for the waves considered here, but the argument can be modified to account for more complex situations. The ADCP beams are oriented with the cardinal directions, so that beams 1 and 2 are directed W and E, respectively, and form an angle θ with the vertical, and the instrument is looking upward without tilt or roll.

The standard transformation that gives the horizontal and vertical components in terms of the eastward (R_2) and westward (R_1) looking beam is

$$\begin{aligned} u_m(z_0, t) &= \frac{[R_2(z_0, t) - R_1(z_0, t)]}{(2\sin\theta)} = u_o + u_a(z_0)\frac{f[k(x_0 + Vt)] + f[k(-x_0 + Vt)]}{2} + w_a(z_0)\frac{g[k(x_0 + Vt)] - g[k(-x_0 + Vt)]}{2\tan\theta} \\ &= u_o + u_a(z_0)\left[f(kVt) + f''(kVt)\frac{(kx_0)^2}{2} \right] + \frac{w_a(z_0)}{\tan\theta} g'(kVt)(kx_0) + o[(kx_0)^3] \\ w_m(z_0, t) &= \frac{[R_2(z_0, t) + R_1(z_0, t)]}{(2\cos\theta) = u_a(z_0)}\frac{f[k(x_0 + Vt)] - f[k(-x_0 + Vt)]}{2}\tan\theta + w_a(z_0)\frac{g[k(x_0 + Vt)] + g[k(-x_0 + Vt)]}{2} \\ &= w_a(z_0)\left[g(kVt) + g''(kVt)\frac{(kx_0)^2}{2} \right] + u_a(z_0)\tan\theta f'(kVt)(kx_0) + o[(kx_0)^3]; \end{aligned} \quad (2)$$

$x_0 = z_0 \tan\theta$ being the distance separating the beams from the vertical axis at distance z_0 from the instrument. Local homogeneity requires thus that $kx_0 = kz_0 \tan\theta \ll 1$. The main source of error is a contamination of one velocity component with the other. Since the standard transformation is a linear combination of time series, low-pass filtering of the beam velocities will remove the error, provided that $g(t)$ and $f(t)$ are contained in the high-frequency section of the spectrum. Thus, the standard transformation is appropriate when the local homogeneity condition applies in the frequency range of interest. For typical mode-1 internal solitary waves, where $w_a(z)$ peaks slightly beneath the pycnocline, Eqs. (2) show that the largest errors are to be expected near the pycnocline in the horizontal velocity. The errors decrease with increasing wavelength. Experiments with synthetic fields show that the error becomes negligible when the beam separation becomes 10% or less of the wavelength. The same experiments also highlight the deceitful nature of the error, since the output of Eqs. (2) appears to fluctuate regularly with "normal" looking amplitude and phase.

3. Comparison of ADCP and pointwise current measurements in MBIWE98

During MBIWE98 currents were measured by a bottom-mounted RD Instrument 300-kHz ADCP, by FSI ACMs, and by VMCMs at a location in the center of Massachusetts Bay in water 85 m deep (site B; Fig. 1). The ADCP pitch and roll remained within 0.6° of the vertical, and the heading did not fluctuate more than 0.3° during the entire month-long deployment, which justifies the assumptions made in the analysis outlined above. The ADCP averaged sixty 1-s samples internally in back-to-back 1-min intervals, and saved the results in beam coordinates. Although the FSIs, VMCMs, and ADCP were not located on the same mooring, the distances separating them was less than 500 m and the velocities were expected to be highly correlated with a phase lag caused by the finite velocity of propagation of the internal waves between the measurement sites.

In Massachusetts Bay, the currents are dominated by the barotropic and baroclinic internal tides, which have horizontal wavelengths much larger than the water depth (85 m) at the site, and by large high-frequency, short-wavelength internal waves (SWIWs) that have typical wavelengths of 200–300 m (Fig. 2). The SWIWs occur in packets containing 5–10 oscillations that propagate southwestward across the bay. At a given location, SWIWs are present for up to 2 h during a tidal cycle and arrive on average every 12.4 h. Forty-six packets of SWIWs were observed during the 4-week experiment. During periods when the SWIWs are absent, the ADCP and pointwise instruments are highly correlated in magnitude and direction, as expected. During periods when the SWIWs are present, the agreement between the ADCP and point current meters is poor (Fig. 3). The largest discrepancies are found at a depth of 20 m, the depth of the pycnocline. The ADCP error velocity is large during times of SWIWs, and generally increases with distance from the instrument, flagging periods when the currents reported by the ADCP are not internally consistent.

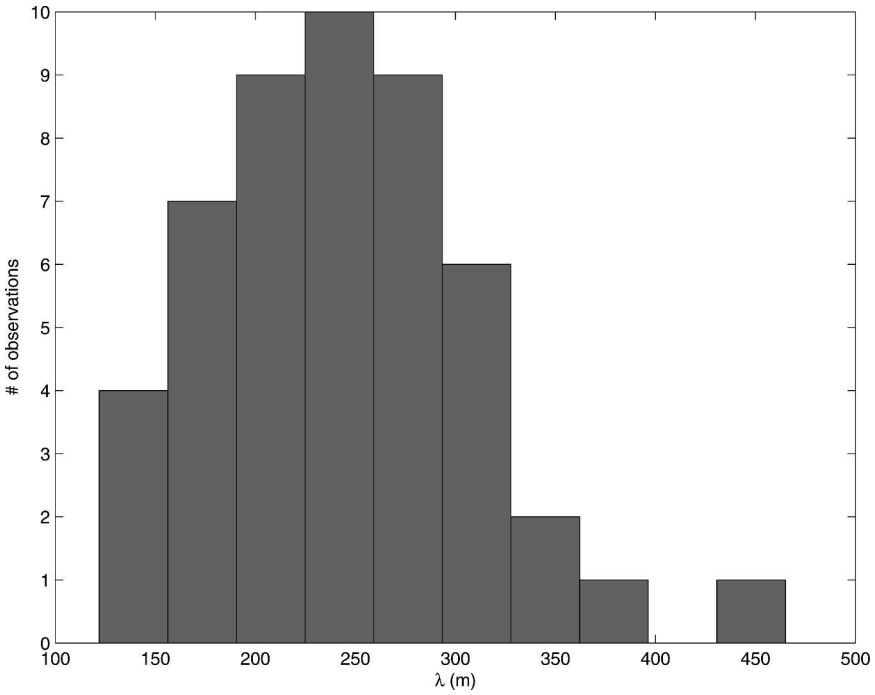

FIG. 2. Observed distribution of wavelengths in packets of SWIWs observed in Massachusetts Bay during MBIWE98. These wavelengths were computed using the array of instruments deployed at site B (Fig. 1).

4. Phase-lagged beam-to-earth transformation: ADCP as SWIW antenna

The ADCP fails to correctly determine the components of the velocity in earth coordinates because the standard algorithm combines beam components that, at a given time, are sampling different phases of the wave. However, the individual velocity measurements in beam coordinates are uncorrupted. Moreover, in the Massachusetts Bay case, SWIWs maintain their coherency over times that are long compared to the few minutes it takes a section of the wave to move 50–100 m from one beam to the opposite beam.

The mismatch in timing of the beam measurements can be corrected by introducing a lagged beam-to-earth transformation:

$$u_m = [R_2(t - s/2) - R_1(t + s/2)]/[2\sin(\theta)],$$
$$w_m = [R_2(t - s/2) + R_1(t + s/2)]/[2\cos(\theta)], \quad (3)$$

where s is the time required by a wave front to move from one beam to the opposite. In our simplified example, $s = 2z_0 \tan\theta/V$. More generally, for a wave propagating at an arbitrary angle ψ relative to the line joining opposite beams, the lag is $s = 2z_0 \tan\theta/V \cos\psi$. In this lagged transformation, the beam velocities corresponding to the same phase in the passing wave are combined to produce the velocity estimates in earth coordinates.

Application of the lagged transformation requires knowledge of the speed of the passing waves. The spreading beams can be used as elements of a directional antenna to compute the celerity of the SWIWs, thus determining s in Eq. (3), in analogy to the way an ADCP can be used in shallow water to determine the propagation spectrum of surface waves (RDI 2000). In the latter application, the displacement of the surface provides an ideal marker to measure speed and propagation direction. For our case, we need to select a different marker. In Massachusetts Bay, we found that the passage of the waves modulates the intensity of the backscatter signal at a given depth, so that for beam n the intensity can be written as

$$e_n(t) = e(t + \tau_{nm}) + \varepsilon_n(t), \quad (4)$$

where τ_{nm} is the antisymmetric matrix of the phase lags of beam n measured relative to beam m and $\varepsilon_n(t)$ represents noise, assumed to be uncorrelated in time and space; that is, $\langle \varepsilon_n(t)\varepsilon_m(t')\rangle = \delta_{m,n}\delta(t - t')$. The modulation in backscatter intensity can be due to different causes, such as shear-generated turbulence, displacement of planktonic scattering layers, or other factors (Chereskin 1983; Sandstrom and Oakey 1995; Apel et al. 1997). However, the only assumption required to use this signal to compute the celerity is that it is due to the passage of the waves, hence traveling at the same phase speed. Ultimately, this assumption needs to be validated a posteriori with an independent estimate of the celerity. For example, in Massachusetts Bay, using a 300-kHz ADCP, the passage of the waves caused the

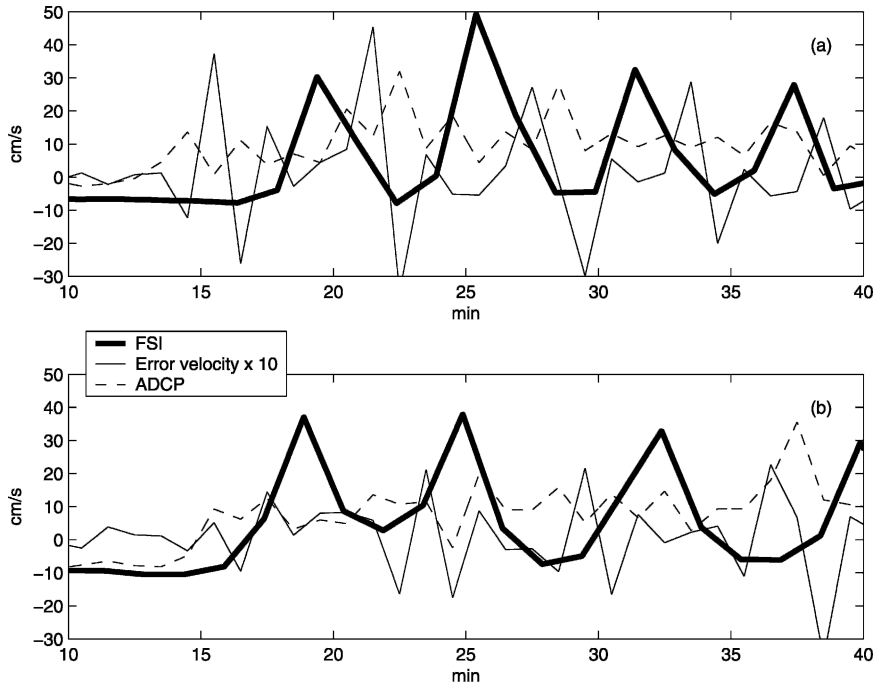

FIG. 3. Two examples of time series of currents measured by a current meter (FSI) located 20 m below the surface (thick line) and by the bottom-mounted ADCP (computed using the standard beam-to-earth transformation) at the same depth (dashed line) during the passage of SWIWs. The currents are rotated in the direction of propagation of the waves (plus is flow toward the southwest, minus is flow toward the northeast). The FSI and ADCP measured time series should be very similar, but shifted by a few minutes because of the spatial separation of the instruments. However, the well-defined southwestward (onshore) pulses in the FSI-measured current associated with the passage of the SWIWs are virtually absent in the ADCP-measured current. Large fluctuations in the error velocity (thin line) computed for the ADCP indicate times when the difference between vertical velocities, measured combining opposite pairs of beams, are large and the horizontal velocities computed using the standard transformation are unreliable.

backscatter at 20 m to periodically increase 20% or more (Fig. 4). Then, the cross-correlation function $\langle (e_n(t) - \langle e_n \rangle)(e_m(t + s) - \langle e_m \rangle) \rangle$ peaks at $s = -\tau_{mn}$ when the interval under consideration contains a train of SWIWs (Jenkins and Watts 1968) (Fig. 4). With the present dataset, cross correlations were calculated over 2-h intervals with SWIWs present, on the assumption that the waves in a single train propagate in the same direction. Although only two lags are necessary to compute celerity and direction of propagation, here we have used all six independent entries in τ_{mn} to minimize the quadratic error:

$$E = \sum_{i>j} [\tau_{ij} V - \Delta x_{ij} \cos(\theta - \psi_{ij})]^2, \qquad (5)$$

where V is the celerity; θ the direction of propagation; and Δx_{ij} and ψ_{ij} are, respectively, the distances and angles between pairs of beams.

5. Application to MBIWE98

To test the celerity calculation using the ADCP backscatter observations, we used the array of instruments deployed during MBIWE98 at site B to derive an independent measure of the wave propagation direction and speed. To evaluate the cross-correlation function, we interpolated the 1-min-averaged ADCP measurements to create a 1-s ADCP time series covering each SWIW wave train (typically lasting 2 h). The resulting estimates for celerity and direction of propagation correlate well with the estimates derived from the larger moored array antenna (Fig. 5). The spreading is consistent with the possibility that the wave fronts are not exactly straight (Trask and Briscoe 1983). On average, the normalized error $\sqrt{E}/\Sigma_{i>j} \Delta x_{ij}$ was less than 5%.

With the lags known, we used the lagged transformation [Eq. (3)] to determine the currents. The improvement in the ADCP currents is remarkable (Fig. 6). The correction is largest for the horizontal velocity, as the phase-lagged transformation removes a term proportional to $(\tan\theta)^{-1} \sim \theta^{-1}$ for the horizontal component, while for the vertical component the contamination is proportional to $\tan\theta \sim \theta$. The improvement is less pronounced when the wavelength of the internal waves is larger and/or the pulses are spread farther apart.

Another measure of the current accuracy is the magnitude of the error velocity, defined as the difference

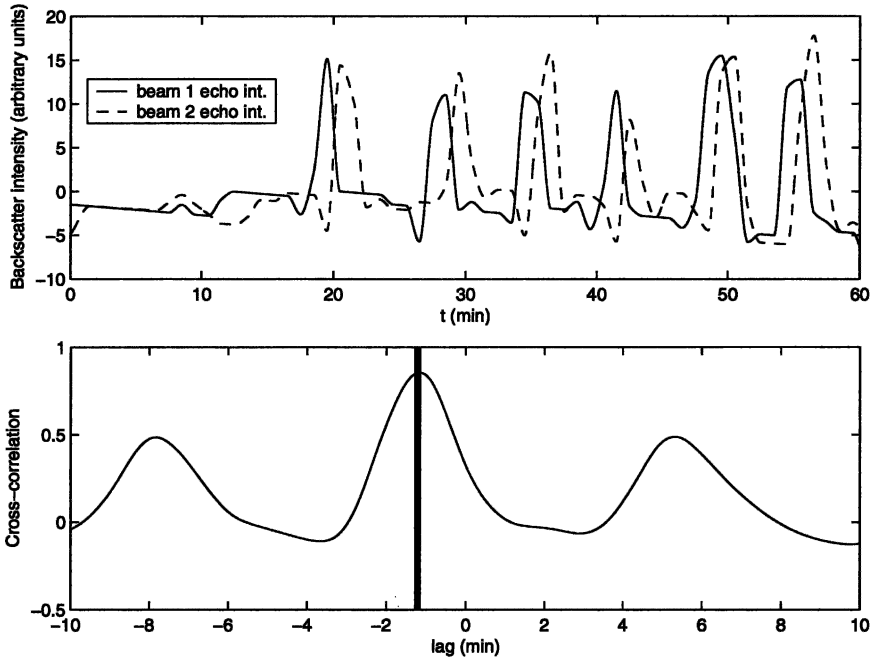

FIG. 4. (top) Time series of backscatter intensity from two opposite beams during the passage of a train of SWIWs in Massachusetts Bay. (bottom) The cross-covariance function of the two backscatter intensity signals shown above. The abscissa of the maximum (marked with the thick vertical line) gives the lag between the signals.

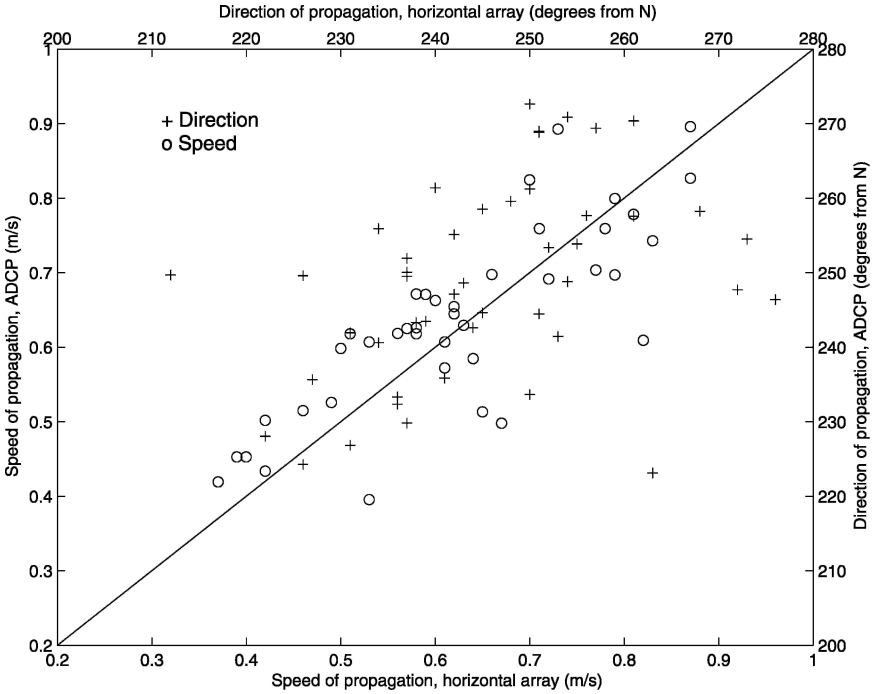

FIG. 5. Scatterplot of wave speed (circles) and direction (crosses) measured by the horizontal array (abscissa) and from the correlation of the backscatter intensity recorded by the ADCP beams (ordinate).

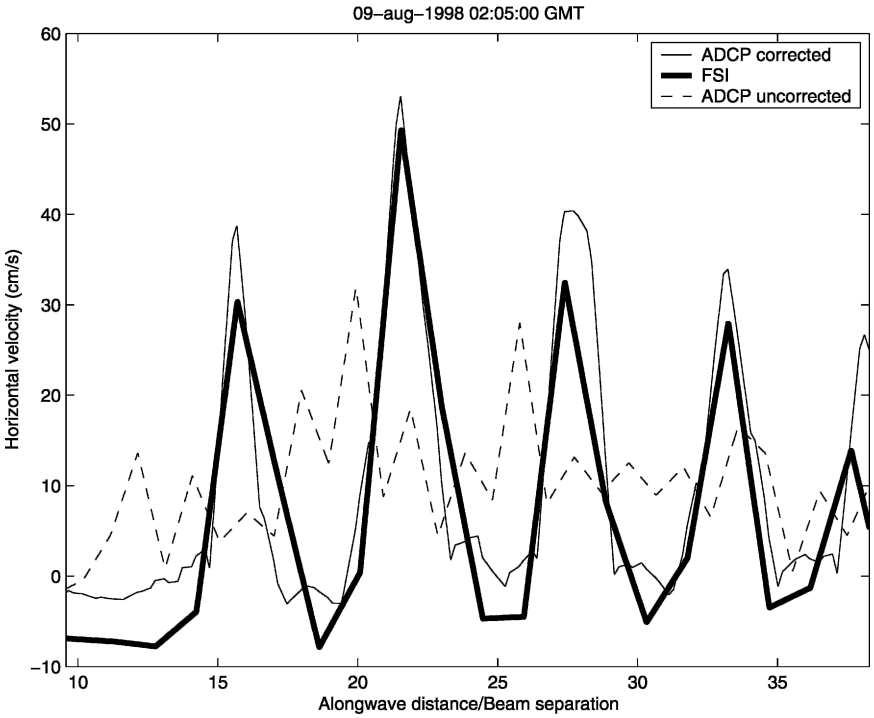

FIG. 6. Comparison of ADCP currents at 20 m computed using the standard (dashed line) and phase-lagged (thin line) method during the passage of a packet of SWIWs at site B in Massachusetts Bay on 9 Aug 1998. For comparison, the thick line shows the current measured by an FSI current meter located about 500 m to the NE at the same depth. The high-pass-filtered currents are rotated to be in the direction of propagation of the wave. The time variable has been transformed into a space variable using the celerity. The x axis represents distance along the wave track normalized by the beam separation. The packet is the same depicted in Fig. 3a.

between the vertical velocities computed using beams 1 and 2 and beams 3 and 4. During non-SWIWs periods, the magnitude of the error velocity is usually small, of the order of 5 mm s^{-1} or less. With SWIW present, the error velocity can be an order of magnitude higher, or about 30% of the vertical velocities observed. Indeed, this observation alone should be enough to question the validity of the standard transformation. Over the 46 packets of SWIWs considered, the application of the phase-lagged transformation reduced the magnitude of the error velocity by 50% or more in 60% of the packets observed at 20 m. The vertical structure of the reduction in error magnitude (Fig. 7) shows that in the upper part of the water column, the magnitude of the error velocity is reduced on average by 45%–55%.

6. Discussion and conclusions

The standard beam-to-earth coordinate transformation used to convert ADCP signals into current time series fails to give a physically meaningful output when the horizontal scale of the currents becomes comparable to the horizontal beam separation. These periods are flagged by the error velocity computed by the ADCP. Since the beam separation is a function of distance from the instrument, a simple criterion is that the horizontal scale should be at least 10 times larger than the vertical extent of the current measurement. Where internal waves with a simple vertical modal structure are the principal cause of the horizontal variability in the current field, we have developed a modified beam-to-earth transformation that utilizes paired beam measurements appropriately lagged to obtain two observations at the same phase of a passing internal wave. This lagged transformation is appropriate when the horizontal length scale is small and the signal remains coherent over the time it takes the wave to pass through the ADCP beam array (in this case, a few minutes).

To illustrate this approach, we compared ADCP and point current measurements obtained in Massachusetts Bay in summer when large SWIWs that violate the local homogeneity condition were present. As expected, the application of the standard beam-to-earth transformation failed when the SWIWs were present (the ADCP observations were in good agreement with pointwise measurements during times when the SWIWs were not present). The alternative phase-lagged earth-to-beam transformation gave currents that compared well with

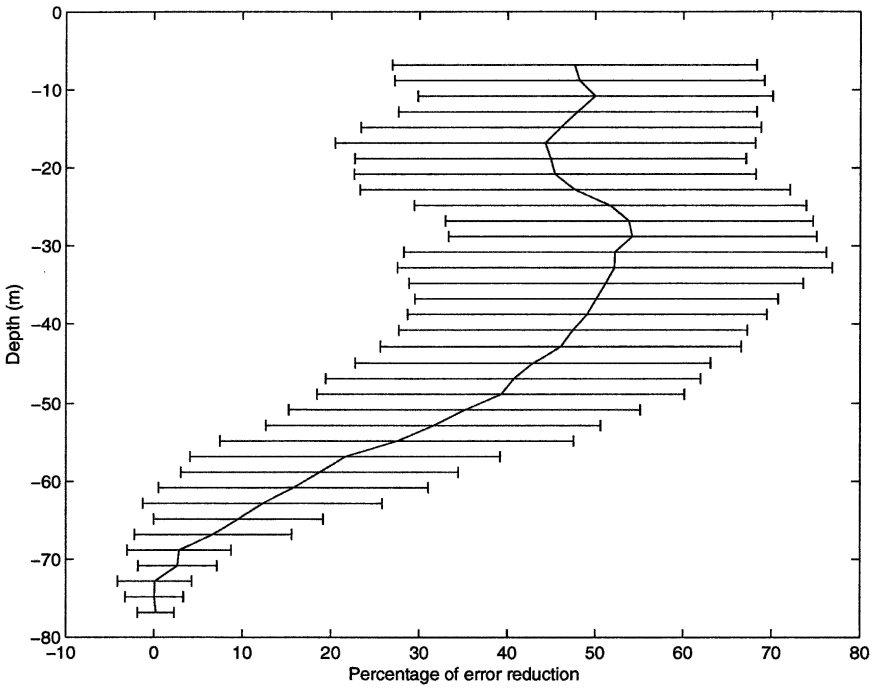

FIG. 7. Vertical structure of the mean reduction in the error velocity magnitude obtained by applying the phase-lagged transformation, averaged over the 46 packets.

the reference pointwise measurements, despite the fact that the ADCP data were averaged over back-to-back 1-min intervals. The modified transformation relies on prior knowledge of the celerity of the passing wave. In the case of the Massachusetts Bay observations, the ADCP can be used as a directional antenna to determine the propagation characteristic. The cross correlation of the backscatter intensity was used to estimate the passage time of the wave fronts at the four beams and, thus, the speed and direction of propagation.

The present dataset shows that even with internal averaging of the order of 20% of the period of the waves we were able obtain meaningful results. Of course, to decrease the error in the estimate of the lags it would be advisable to reduce as much as possible, when storage is not an issue, the internal averaging interval, especially if there is no a priori knowledge of the period of the waves.

The Massachusetts Bay observations present a special situation where the internal waves are sufficiently large and organized to utilize the alternate beam-to-earth lagged transformation presented here. There are also situations where the passage of the SWIWs does not affect the backscatter intensity sufficiently to allow determination of the wave speed and propagation direction. In this case, other solutions should be attempted, possibly based on the statistical analysis of the beam velocities themselves.

Acknowledgments. A. Scotti was partially supported by ONR Grants N00014-03-1-0553 and N00014-01-1-0172, B. Butman and P. Alexander by the U.S. Geological Survey, and R. Beardsley by the WHOI Smith Chair and ONR Grant N00014-98-1-0210. S. Anderson received partial support from ONR (Grant N00014-97-1-0158). The Massachusetts Bay Internal Wave Experiment was jointly supported by ONR and USGS. We acknowledge the many WHOI and USGS scientists, engineers, and technicians who conducted the MBIWE98. We also thank J. Bane (UNC), H. Seim (UNC), and A. Pluddemann (WHOI) for interesting and helpful discussions.

REFERENCES

Apel, J. R., and Coauthors, 1997: An overview of the 1995 SWARM shallow-water internal wave acoutstic scattering experiment. *IEEE J. Oceanic Eng.,* **22,** 465–500.

Chereskin, T. K., 1983: Generation of internal waves in Massachusetts Bay. *J. Geophys. Res.,* **88,** 2649–2661.

Colosi, J. A., R. C. Beardsley, J. F. Lynch, G. Gawarkiewicz, C.-S. Chiu, and A. Scotti, 2001: Observation of nonlinear internal waves on the New England continental shelf during Summer Shelfbreak Primer study. *J. Geophys. Res.,* **106,** 9587–9601.

Gargett, A. E., 1994: Observing turbulence with a modified Acoustic Doppler Current Profiler. *J. Atmos. Oceanic Technol.,* **11,** 1592–1610.

Holloway, P. E., P. G. Chatwin, and P. Craig, 2001: Internal tide observations from the Australian West Shelf in summer 1995. *J. Phys. Oceangr.,* **31,** 1182–1199.

Holt, J. T., and S. A. Thorpe, 1997: The propagation of high-frequency internal waves in the Celtic Sea. *Deep-Sea Res.,* **44,** 2087–2116.

Jenkins, G. M., and D. G. Watts, 1968: *Spectral Analysis and Its Applications.* Holden-Day, 525 pp.

Liu, A. K., Y. S. Chang, M.-K. Hsu, and N. K. Liang, 1998: Evolution of nonlinear internal waves in the East and South China Seas. *J. Geophys. Res.,* **103,** 7995–8008.

New, A. L., and R. D. Pingree, 1992: Local generation of internal soliton packets in the central Bay of Biscay. *Deep-Sea Res.,* **39,** 1521–1534.

Polzin, K. E., E. Kunze, J. Hummon, and E. Firing, 2002: The finescale response of a lowered ADCP velocity profiler. *J. Atmos. Oceanic Technol.,* **19,** 205–224.

RDI, 2000: *Workhorse ADCP Multi-Directional Wave Gauge Primer.* RD Instruments, 8 pp.

Sandstrom, H., and N. S. Oakey, 1995: Dissipation in internal tides and solitary waves. *J. Phys. Oceanogr.,* **25,** 604–614.

Small, J., T. C. Sawyer, and J. C. Scott, 1999: The evolution of an internal bore at the Malin shelf break. *Ann. Geophys.,* **17,** 547–565.

Trask, R. P., and M. G. Briscoe, 1983: Detection of Massachusetts Bay internal waves by the synthetic aperture radar (SAR) on SEASAT. *J. Geophys. Res.,* **88,** 1789–1799.

Trevorrow, M. V., 1998: Observations of internal solitary waves near the Oregon coast with an inverted echo sounder. *J. Geophys. Res.,* **103,** 7671–7680.